MOLECULAR PLANT PATHOLOGY (2008) **9**(3), 339–355 DOI: 10.1111/J.1364-3703.2008.00470.X

Indole-3-acetic acid (IAA) biosynthesis in the smut fungus *Ustilago maydis* and its relevance for increased IAA levels in infected tissue and host tumour formation

GAVIN REINEKE[1], BERNADETTE HEINZE[1], JAN SCHIRAWSKI[1], HERMANN BUETTNER[2], REGINE KAHMANN[1] AND CHRISTOPH W. BASSE[1,*]

[1] *Max-Planck-Institute for Terrestrial Microbiology, Department of Organismic Interactions, Karl-von-Frisch-Strasse, D-35043 Marburg, Germany*
[2] *University of Applied Sciences Münster, Stegerwaldstrasse 39, D-48565 Steinfurt, Germany*

SUMMARY

Infection of maize (*Zea mays*) plants with the smut fungus *Ustilago maydis* is characterized by excessive host tumour formation. *U. maydis* is able to produce indole-3-acetic acid (IAA) efficiently from tryptophan. To assess a possible connection to the induction of host tumours, we investigated the pathways leading to fungal IAA biosynthesis. Besides the previously identified *iad1* gene, we identified a second indole-3-acetaldehyde dehydrogenase gene, *iad2*. *Δiad1Δiad2* mutants were blocked in the conversion of both indole-3-acetaldehyde and tryptamine to IAA, although the reduction in IAA formation from tryptophan was not significantly different from *Δiad1* mutants. To assess an influence of indole-3-pyruvic acid on IAA formation, we deleted the aromatic amino acid aminotransferase genes *tam1* and *tam2* in *Δiad1Δiad2* mutants. This revealed a further reduction in IAA levels by five- and tenfold in mutant strains harbouring the *Δtam1* and *Δtam1Δtam2* deletions, respectively. This illustrates that indole-3-pyruvic acid serves as an efficient precursor for IAA formation in *U. maydis*. Interestingly, the rise in host IAA levels upon *U. maydis* infection was significantly reduced in tissue infected with *Δiad1Δiad2Δtam1* or *Δiad1Δiad2Δtam1Δtam2* mutants, whereas induction of tumours was not compromised. Together, these results indicate that fungal IAA production critically contributes to IAA levels in infected tissue, but this is apparently not important for triggering host tumour formation.

INTRODUCTION

The basidiomycete *Ustilago maydis* is a member of the smut fungi whose estimated 1200 species cause worldwide diseases in over 75 plant families of the angiosperms. *U. maydis* is a genetically well-characterized model organism and its genome sequence has recently been published (Basse and Steinberg, 2004; Kämper *et al.*, 2006). *U. maydis* differs from other smut fungi in its ability to incite tumours in all aerial parts of its host plants maize (*Zea mays*) and teosinte (*Zea mays* ssp. *parviglumis*). Under natural conditions tumours are frequently observed in reproductive organs and preferentially develop within kernels. At advanced stages of the infection they become filled with billions of sexual teliospores (Christensen, 1963; Kahmann *et al.*, 2000; Kämper *et al.*, 2006; Martínez-Espinoza *et al.*, 2002). The association of tumour development with plant cell enlargement and proliferation suggested an involvement of phytohormones (Banuett and Herskowitz, 1996; Callow and Ling, 1973; Doehlemann *et al.*, 2007; Kahmann *et al.*, 2000; Snetselaar and Mims, 1994). In particular, markedly elevated indole-3-acetic acid (IAA) levels in tumour tissue relative to non-infected control tissue as well as the ability of *U. maydis* to efficiently convert exogenously added tryptophan (Trp) to IAA have pointed to a role of fungal IAA production in tumour induction (Basse *et al.*, 1996; Moulton, 1942; Sosa-Morales *et al.*, 1997; Turian and Hamilton, 1960; Wolf, 1952).

In plants, several IAA biosynthesis pathways starting from Trp have been proposed, but only a few biosynthesis genes have been identified and characterized (Woodward and Bartel, 2005). The indole-3-pyruvic acid (IPA) pathway is initiated by the oxidative transamination of Trp to IPA and proceeds via indole-3-acetaldehyde (IAAld) to IAA through the activities of IPA decarboxylase and IAAld dehydrogenase, respectively (Fig. 1). In Arabidopsis (*Arabidopsis thaliana*) and tomato, IPA has been detected and in *Lupinis albus* and *Medicago truncatula,* IAAld dehydrogenase activities have been identified (Cooney and Nonhebel, 1989; Fedorova *et al.*, 2005; Spaepen *et al.*, 2007; Tam and Normanly, 1998). IAAld as the terminal intermediate of IAA biosynthesis may also arise from tryptamine (TAM) via the intermediate indole-3-acetaldoxime (IAOx) (Fig. 1; Zhao *et al.*,

* *Correspondence*: Tel.: +49 6421 178 600; Fax: +49 6421 178 609;
E-mail: basse@ mpi-marburg.mpg.de

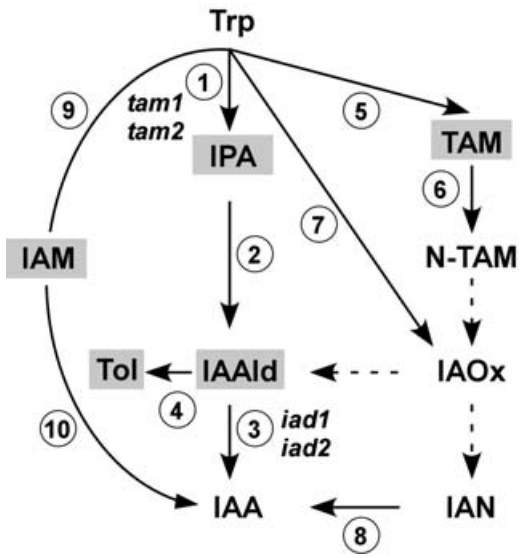

Fig. 1 Trp-dependent IAA biosynthesis. The scheme shows IAA pathways and key intermediates proposed for plants and microorganisms. Trp, tryptophan; IPA, indole-3-pyruvic acid; IAAld, indole-3-acetaldehyde; IAA, indole-3-acetic acid; Tol, indole-3-ethanol; TAM, tryptamine; N-TAM, N-hydroxyl tryptamine; IAOx, indole-3-acetaldoxime; IAN, indole-3-acetonitrile; IAM, indole-3-acetamide. Enzymes involved in these pathways are: Trp aminotransferase (1), IPA decarboxylase (2), IAAld dehydrogenase (3), IAAld reductase (4), Trp decarboxylase (5), flavin monooxygenase-like enzymes (6), cytochrome P450 enzymes (7); nitrilase (8); Trp monooxygenase (9); IAM hydrolase (10). Possible intermediates or by-products of IAA formation thus far reported for fungi are shaded grey (see Discussion). Enzymes for the conversion of intermediates connected by dashed arrows are elusive. *U. maydis* genes involved in IAA formation are indicated. Tol emerges as a by-product from IAAld in the absence of IAAld dehydrogenase activity.

2001, 2002). In support of a pathway via TAM, members of the *YUC* gene family, which encode flavin monooxygenase-like enzymes converting TAM to N-hydroxyl tryptamine, play an important role in IAA formation (Cheng *et al.*, 2006; Zhao *et al.*, 2001). Alternatively, IAOx can be directly generated from Trp and thus bypass TAM formation. In Arabidopsis, two corresponding P450 monooxygenase activities have been identified, which are relevant for IAA biosynthesis (Hull *et al.*, 2000; Mikkelsen *et al.*, 2000; Zhao *et al.*, 2002). Evidence exists that indole-3-acetonitrile (IAN) as well as IAAld may be intermediates in IAA biosynthesis from IAOx (Bak *et al.*, 2001; Barlier *et al.*, 2000 and references therein). Besides IAA formation via the precursors IAN or IAAld, Trp can be converted to IAA via indole-3-acetamide through the consecutive activities of Trp monooxygenase and indole-3-acetamide hydrolase, as reported for some plant-associated bacteria (Fig. 1; Spaepen *et al.*, 2007; Yamada *et al.*, 1985). Such a pathway has also been suggested to exist in Arabidopsis based on the occurrence of indole-3-acetamide (IAM) and an IAM hydrolase activity encoded by the *AMI1* gene (Pollmann *et al.*, 2002, 2003). In addition to the IAM pathway, IAA formation via the IPA pathway has been described in a broad range of bacterial species, underlining the occurrence of IPA as an auxin source (Spaepen *et al.*, 2007). In fungi, although a variety of intermediates in IAA biosynthesis have been proposed, corresponding biosynthesis genes have not yet been addressed except for the *U. maydis iad1* gene (see below and Discussion).

We have re-investigated IAA biosynthesis from Trp in *U. maydis* to address a possible role in host tumour formation. The previously identified *U. maydis iad1* gene encodes a NAD-dependent IAAld dehydrogenase (Basse *et al.*, 1996). *U. maydis Δiad1* mutants are blocked in IAA formation from IAAld in glucose-containing medium; however, IAA formation was partially regained in medium with arabinose as the carbon source. This led us to propose the existence of a second IAAld dehydrogenase, termed Iad2, which should be subject to glucose-repression. Furthermore, the efficient conversion of TAM to IAA in glucose-free medium suggested a participation of Iad2 (Basse *et al.*, 1996). In addition, we have observed IPA accumulation from Trp in glucose-containing medium (Basse *et al.*, 1996), raising the question of whether IPA plays a role in IAA formation.

In this report, we describe for the first time the identification of fungal genes efficiently contributing to Trp-dependent IAA biosynthesis. *U. maydis* mutants strongly affected in IAA biosynthesis were generated and analysed with regard to tumour induction and the ability to cause elevated IAA levels in infected host tissue. This allowed us to separate fungal IAA production from host tumour formation.

RESULTS

Identification of *Iad2*

In order to identify the second IAAld dehydrogenase gene *iad2*, we searched for potential aldehyde dehydrogenase (*pad*) genes displaying sequence similarity to *iad1* and a carbon source-dependent expression profile. The *pad2* and *pad3* genes (MIPS annotation nos um03523 and um10596), whose deduced amino acid sequences display 53 and 52% identity to Iad1, respectively, were retrieved by Southern blot hybridization with *iad1* as probe and chromosomal DNA of *Δiad1* mutants. However, *pad2* and *pad3*, which encode the closest homologues of Iad1 among all 16 additional aldehyde dehydrogenases predicted by the MIPS annotation of the *U. maydis* genome, were not upregulated in complete medium (CM) in the presence of arabinose (CM/Ara) compared with glucose-containing CM (CM/Glc; data not shown). A PCR approach with oligonucleotides deduced from regions conserved between Iad1 and fungal aldehyde dehydrogenases led to the identification of *pad5* (see Experimental procedures). Northern blot analysis revealed that *pad5* is expressed in CM/Ara as well as in CM without an additional carbon source, whereas

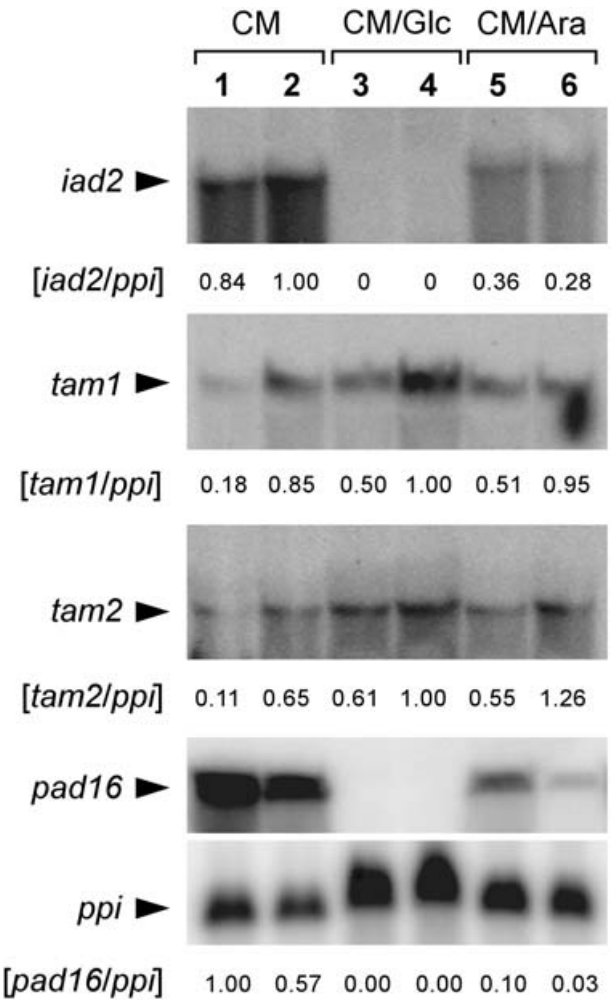

Fig. 2 Carbon source-dependent expression of *iad2*, *tam1*, *tam2* and *pad16*. *U. maydis* strains FB1 (lanes 1, 3, 5) and FB2 (lanes 2, 4, 6) were cultivated in either CM without an additional carbon source (CM), CM/Glc or CM/Ara. For RNA-blot analysis, total RNA (about 10 μg per lane for *iad2*, *tam1* and *tam2*, and about 40 μg per lane for *pad16*) was loaded, and hybridized with the ^{32}P-labelled probes as indicated. Radioactive signals were quantified. Filters were additionally hybridized with the constitutively expressed *ppi* gene (shown for *pad16*) to calculate the ratios of gene-specific to *ppi* signals.

transcripts were not detected in CM/Glc (Fig. 2), indicating that expression of this gene is subject to glucose repression. The predicted ORF of this gene, renamed *iad2*, which after completion of the genome sequence by the Broad Institute was annotated as um03402 by MIPS, encodes a protein of 482 amino acids, with a calculated molecular mass of 53.0 kDa and 36.9% sequence identity to Iad1. The Iad2 sequence also contains the highly conserved amino acid residues described to be involved in catalytic activity, and substrate and cofactor binding (Fig. 3; Yoshida *et al.*, 1998). The absence of a predicted mitochondrial presequence points to a cytosolic localization.

To examine IAAld dehydrogenase activity of Iad2, the corresponding cDNA sequence was expressed as His-tagged fusion in *Escherichia coli* under an arabinose-inducible promoter. The *iad1* gene, its closest homologue, *pad2*, and the *pad16* gene (MIPS annotation no. um03665), which is upregulated in CM/Ara and most strongly expressed in CM without an additional carbon source compared with CM/Glc (Fig. 2), were included as controls. *E. coli* strains carrying the pBADiad1, pBADpad2, pBADiad2 and pBADpad16 expression constructs were denoted GR1, GR2, GR5, and GR16, respectively. Expression of His-tagged proteins of the expected sizes was verified by immunoblot analysis (Fig. 4A), and IAAld dehydrogenase activity was examined *in vitro* (see Experimental procedures). As assessed from treatment of ethyl acetate-extracted reaction products with the Salkowski reagent, which is indicative for IAA formation, positive reactions were confined to extracts from strains GR1 and GR5 grown under promoter-inducing conditions (data not shown). Explicitly, reversed-phase HPLC of reaction products and analysis of fractions with the Salkowski reagent confirmed IAAld dehydrogenase activity in strains GR1 and GR5. In contrast, strain GR2 was devoid of IAAld dehydrogenase activity (Fig. 4B,C). The small IAA peak seen in the GR2 profile (Fig. 4B) was also detected under non-inducing conditions and thus was not a consequence of Pad2 expression (data not shown). *In vitro* analysis of the pH and co-factor requirements of Iad2 revealed a pH optimum of 8 and a clear preference for NAD as co-factor (Fig. 4D). In conclusion, Iad2 functions as NAD-dependent IAAld dehydrogenase.

Loss of IAAld dehydrogenase activity in *Δiad1Δiad2* mutants

To determine the influence of *iad2* on IAA formation and to rule out the existence of additional IAAld dehydrogenase activities, *iad2* was deleted in wild-type and *Δiad1* mutant strains. The resulting strains GRN1 (FB1Δiad2), GRN3 (FB2Δiad2), GRN7 (FB1Δiad1Δiad2) and GRN8 (FB2Δiad1Δiad2) were compared with their parental strains for the ability to convert IAAld to IAA in CM/Ara. Extracts from cell-free supernatants of wild-type and *Δiad2* mutant strains displayed similar Salkowski reactions (Fig. 5A), and the formation of similar IAA amounts was confirmed by HPLC analysis (Fig. 5B; data not shown). As expected from our previous investigation, *Δiad1* mutants were markedly reduced in IAA formation from IAAld (Fig. 5A–C). Strikingly, however, extracts from *Δiad1Δiad2* mutants were almost devoid of IAA as assessed from the weak Salkowski reaction and from HPLC analysis (Fig. 5A–C). Quantitative HPLC analysis documented that IAA levels were reduced > 50-fold in *Δiad1Δiad2* mutants relative to parental *Δiad1* mutant strains in favour of tryptophol (Tol; indole-3-ethanol) formation (Fig. 5B,C). This indicates that Iad1 and Iad2 function as IAAld dehydrogenases

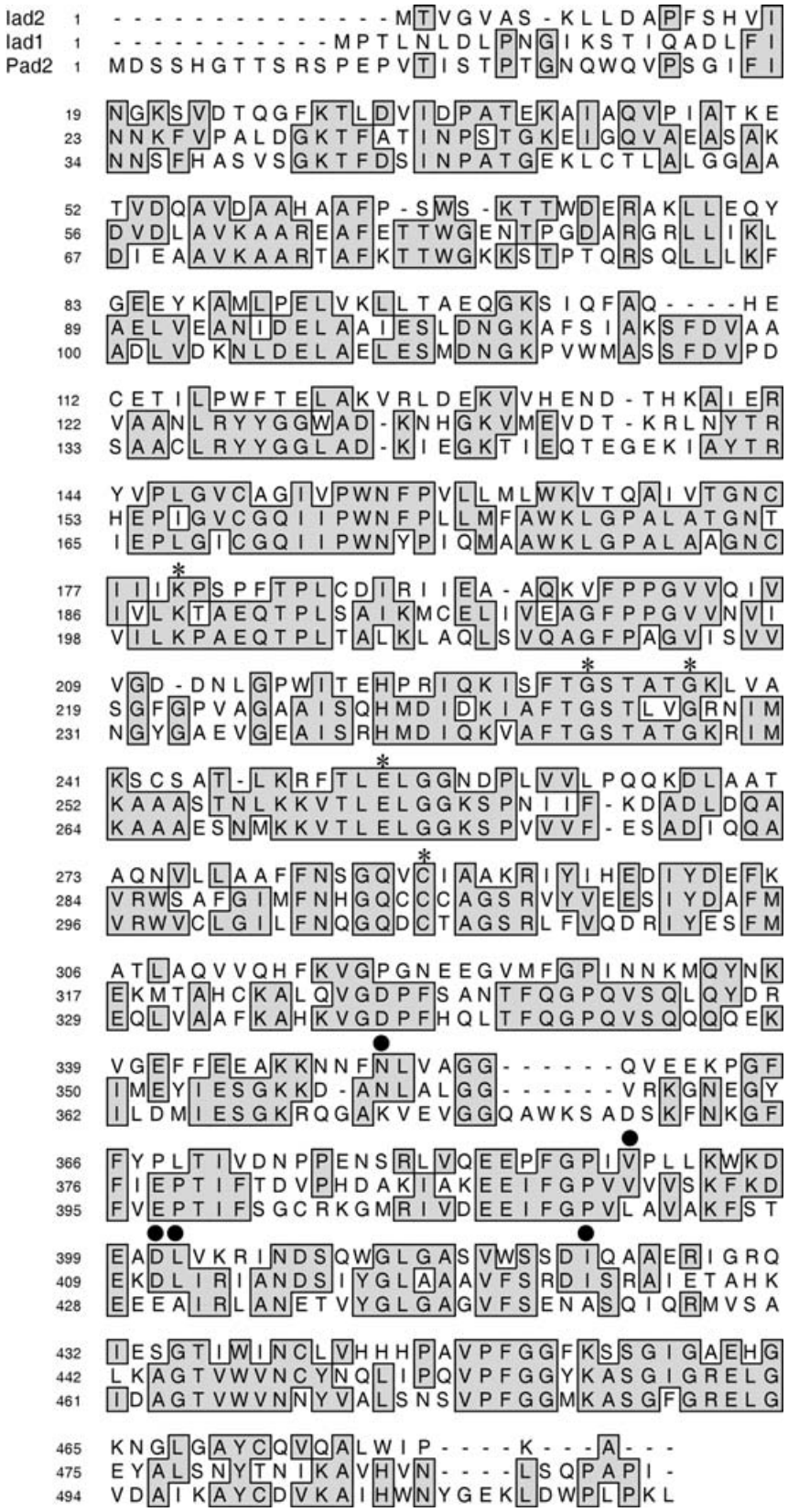

Fig. 3 Sequence alignment of Iad2 with Iad1 and Pad2. Identical amino acids are boxed and shaded. Gaps have been inserted to increase the number of identities. Asterisks mark highly conserved amino acid residues described to be implicated in catalytic activity (E_{253}), substrate binding (C_{288}) and NAD binding (K_{180}, G_{231}, G_{236}; numbers refer to Iad2). Dots mark amino acids shared between Iad1 and Iad2 and absent from all remaining predicted aldehyde dehydrogenase sequences of *U. maydis* (see Discussion).

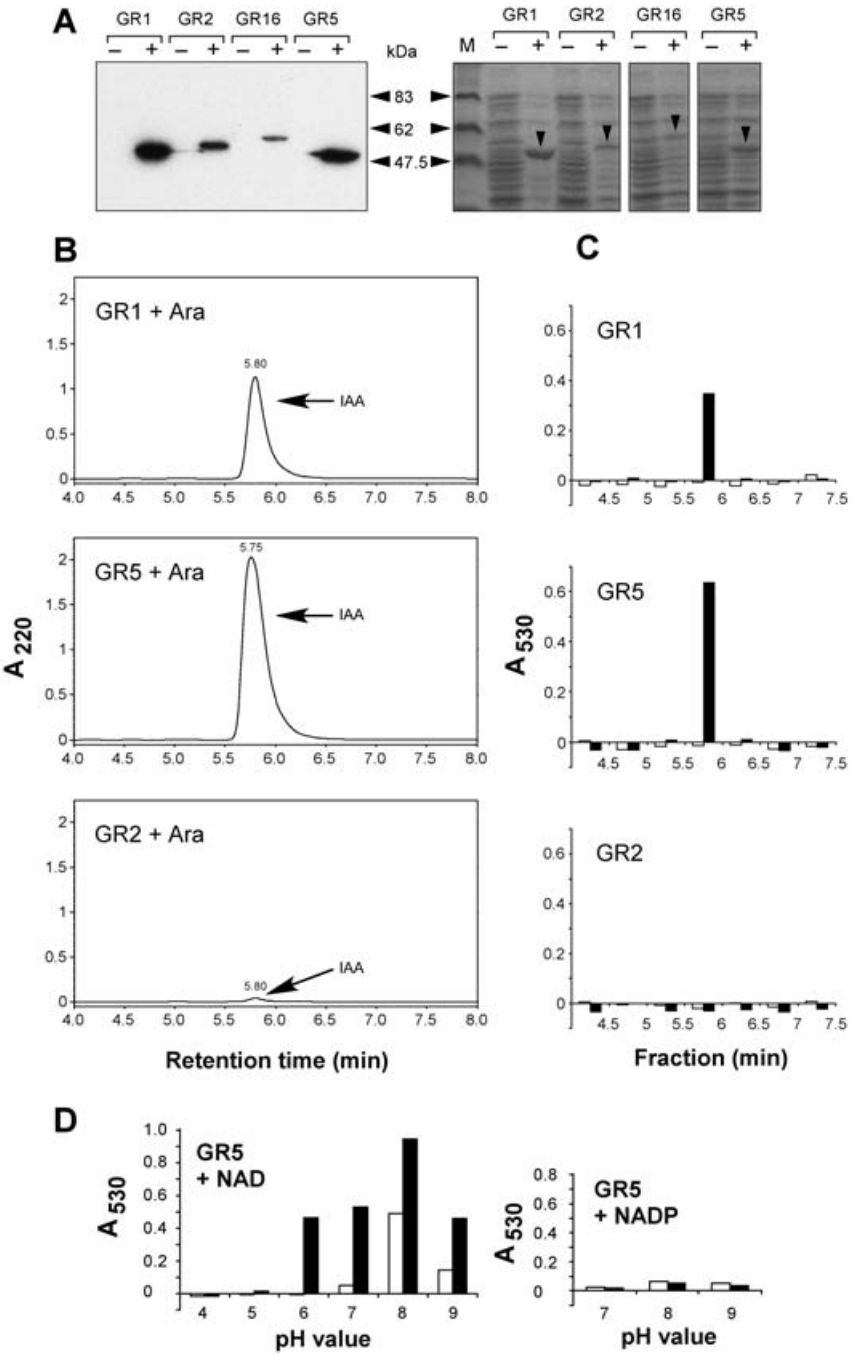

Fig. 4 Demonstration of IAAld activity *in vitro*. (A) Immunoblot analysis of His-tagged proteins expressed in *E. coli* strains GR1 (Iad1; 53.7 kDa), GR2 (Pad2; 56.2 kDa), GR16 (Pad16; 57.4 kDa) and GR5 (Iad2; 53.0 kDa) using an anti-His antibody. Cultures were incubated under non-inducing (–) or inducing conditions (+). Protein amounts corresponding to 40 μL of cell culture were loaded per lane. Size markers are indicated on the right. The right panel shows the Coomassie-stained gel loaded with the same amounts of the same protein preparations. Arrowheads point to the Iad1, Pad2, Pad16 and Iad2 proteins expressed under inducing conditions. M: molecular mass standards. (B) HPLC analysis of *in vitro* reaction products. Identical volumes of enzyme extracts (corresponding to 0.7 mL of cell culture each and 100 μg protein for GR1, 200 μg for GR2 and 400 μg for GR5) prepared from *E. coli* strains GR1, 2 and 5 grown in parallel under inducing conditions (+Ara) were applied for the enzyme assay in the presence of IAAld (0.5 mM). Reaction products were separated by HPLC. The IAAld substrate (elutes 1 min earlier than IAA under the applied conditions) was removed from the samples via ethyl acetate extraction. Absorbance was monitored at 220 nm. Arrows denote peaks eluting like IAA. (C) Salkowski analysis of HPLC fractions. Fractions from HPLC runs of reaction products under non-inducing conditions (open bars) and inducing conditions (closed bars) were collected for detection of IAA with the Salkowski reagent. Absorbance was measured at 530 nm. (D) Co-factor and pH requirements of Iad2. The desalted extract from induced *E. coli* strain GR5 was incubated with IAAld (0.5 mM) in the presence of either NAD (1 mM) (left panel) or NADP (1 mM) (right panel). Reactions were allowed to proceed for 5 min (open bars) or 30 min (closed bars). Products were treated with the Salkowski reagent. Absorbance was measured at 530 nm.

in vivo and excludes the existence of redundant enzyme activities under the tested conditions.

Δiad1Δiad2 mutants are blocked in the conversion of tryptamine to IAA

Previous studies have revealed that exogenously added TAM is efficiently converted to IAA in *U. maydis* grown in CM/Ara (Basse *et al.*, 1996). For this reason, we investigated whether both Iad1 and Iad2 are required for the conversion of TAM to IAA *in vivo*. To discriminate between their contributions, TAM feeding experiments were performed with wild-type, *Δiad1*, *Δiad2* and *Δiad1Δiad2* mutant strains. *Δiad2* mutants were not significantly affected in TAM to IAA conversion compared with wild-type strains (Table 1). In agreement with a previous investigation (Basse *et al.*, 1996), *Δiad1* mutants were significantly reduced in

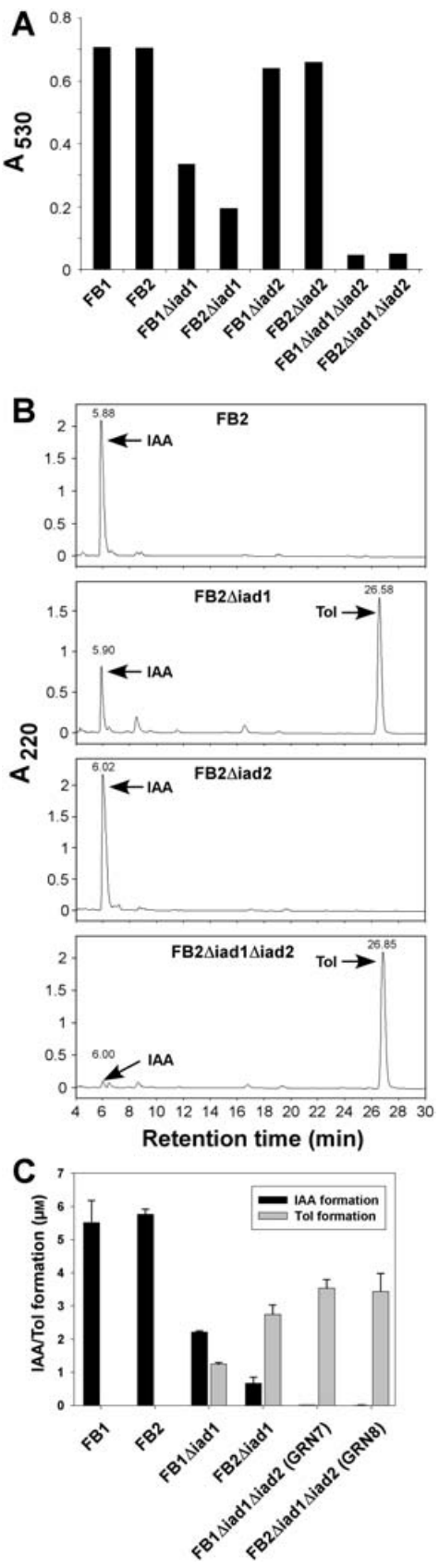

IAA formation from TAM. Interestingly, however, conversion of TAM to IAA was almost eliminated in *Δiad1Δiad2* mutants (Table 1), indicating that TAM is converted to IAA through IAAld dehydrogenase activities of Iad1 and Iad2.

Conversion of Trp to IAA in *Δiad1Δiad2* mutants

We next addressed whether Iad2 plays a role in IAA formation from Trp by comparing wild-type, *Δiad1*, *Δiad2* and *Δiad1Δiad2* mutants cultivated in CM/Ara. In agreement with a previous investigation, *Δiad1* strains exhibited an approximately threefold reduction in the conversion of Trp to IAA, whereas *Δiad2* mutants displayed wild-type-like IAA levels (Table 1). IAA levels were not significantly lower in *Δiad1Δiad2* relative to *Δiad1* mutants (Table 1), suggesting that Iad1 is sufficient for the conversion of IAAld derived from exogenously added Trp.

Identification of the *U. maydis nit1* gene and analysis of IAA formation in *Δiad1Δiad2Δnit1* mutants

To address the existence of an IAAld dehydrogenase-independent IAA pathway in *U. maydis*, we investigated the possibility of IAA formation via IAN. The *U. maydis* genome revealed three predicted nitrilase genes (MIPS annotation nos. um10444, um11973 and um05032). Interestingly, the amino acid sequence deduced from um10444 (*nit1*) is more similar to plant nitrilases than predicted nitrilase family proteins from fungi, with highest similarities to NIT1 and NIT2 from Arabidopsis (≥ 43% identity), which are involved in IAA formation (Normanly *et al.*, 1997; Schmidt *et al.*, 1996). *nit1* was deleted in *Δiad1Δiad2* mutant strains to assess a possible contribution to IAA formation. The resulting strains BH7 (FB1Δiad1Δiad2Δnit1) and BH13 (FB2Δiad1Δiad2Δnit1) were similarly affected in IAA formation from IAAld and TAM as the *Δiad1Δiad2* double mutants (Table 1; data not shown). However, the residual IAA formation from Trp in *Δiad1Δiad2* mutants was not diminished in the absence of *nit1* both in CM/

Fig. 5 IAA and Tol production in *Δiad1*/*Δiad2* mutant strains. (A) Strains FB1, FB2, FB1Δiad1, FB2Δiad1, FB1Δiad2 (GRN1), FB2Δiad2 (GRN3), FB1Δiad1Δiad2 (GRN7) and FB2Δiad1Δiad2 (GRN8) were incubated in the presence of 0.2 mM IAAld, and IAA formation was determined in culture supernatants (150 μL) by the Salkowski reagent. Absorbance was measured at 530 nm. (B) HPLC analysis of extracted culture supernatants from strains FB2, FB2Δiad1, GRN3 and GRN8 cultivated as described in A. Absorbance was monitored at 220 nm. Arrows denote peaks eluting like IAA and Tol, respectively. (C) Quantification of IAA and Tol formation. Extracted culture supernatants from strains FB1, FB2, FB1Δiad1, FB2Δiad1, GRN7 and GRN8 incubated in CM/Ara in the presence of 20 μM IAAld were subjected to HPLC analysis and peak areas were quantified for calculation of IAA and Tol concentrations. The mean (± SD) values were calculated from three replicates of a single strain.

Table 1 Influence of the *Δiad1*/*Δiad2* and *Δnit1* deletions on the *in vivo* conversion of TAM or Trp to IAA.*

	TAM		Trp	
	IAA			
Strain	Mean ± SD (μM)	Mean ± SD (%)	Mean ± SD (μM)	Mean ± SD (%)
FB1	1.58 ± 0.27 (6)	100.0 ± 17.1	0.148 ± 0.025 (4)	100.0 ± 16.9
FB2	2.31 ± 0.60 (6)	146.2 ± 38.0	0.140 ± 0.011 (4)	94.6 ± 7.4
FB1Δiad1	0.28 ± 0.06 (3)	17.7 ± 3.8	0.050 ± 0.015 (4)	33.8 ± 10.1
FB2Δiad1	0.32 ± 0.10 (3)	20.3 ± 6.3	0.039 ± 0.010 (4)	26.4 ± 6.8
FB1Δiad2 (GRN1)	1.05 ± 0.32 (6)	66.5 ± 20.3	0.130 ± 0.014 (4)	87.8 ± 9.5
FB2Δiad2 (GRN3)	3.19 ± 0.31 (6)	201.9 ± 19.6	0.130 ± 0.009 (4)	87.8 ± 6.1
FB1Δiad1Δiad2 (GRN7)	0.04 ± 0.04 (6)	2.5 ± 2.5	0.027 ± 0.010 (4)	18.2 ± 6.8
FB2Δiad1Δiad2 (GRN8)	0.01 ± 0.02 (6)	0.6 ± 1.3	0.033 ± 0.005 (4)	22.3 ± 3.4
GRN7Δnit1 (BH7)	0.03 ± 0.00 (3)	1.9 ± 0.0	0.042 ± 0.001 (4)	28.4 ± 0.7
GRN8Δnit1 (BH13)	0.01 ± 0.02 (3)	0.6 ± 1.2	0.035 ± 0.006 (4)	23.6 ± 4.1

*Strains were incubated in CM/Ara in the presence of 0.5 mM TAM or 5 mM Trp. Concentrations were calculated from peak areas resulting from HPLC analysis. The mean (± SD) values were calculated from three to six replicates (numbers in parentheses) of a single strain.

Table 2 Influence of the *Δtam1*/*Δtam2* deletions on the *in vivo* conversion of Trp to IAA and IPA.

	CM/Glc*				CM/Ara†	
	IAA		IPA		IAA	
Strain	Mean ± SD (μM)	Mean ± SD (%)	Mean ± SD (μM)	Mean ± SD (%)	Mean ± SD (μM)	Mean ± SD (%)
FB1	3.08 ± 0.37	100.0 ± 12.1	844.1 ± 91.5	100.0 ± 10.8	0.220 ± 0.032	100.0 ± 14.5
FB2	2.52 ± 0.42	81.9 ± 13.7	243.6 ± 56.1	28.9 ± 6.6	0.239 ± 0.016	108.6 ± 7.5
FB1Δiad1Δiad2 (GRN7)	2.15 ± 0.33	69.8 ± 11.1	228.9 ± 24.0	27.1 ± 2.8	0.071 ± 0.004	32.3 ± 1.6
FB2Δiad1Δiad2 (GRN8)	1.85 ± 0.19	60.2 ± 6.2	296.9 ± 56.8	35.2 ± 6.7	0.063 ± 0.008	28.5 ± 3.8
GRN7Δtam1‡	0.31 ± 0.07	10.0 ± 2.1	41.6 ± 13.0	4.9 ± 1.5	0.027 ± 0.008	12.3 ± 3.6
GRN8Δtam1‡	0.34 ± 0.07	11.2 ± 2.2	46.7 ± 15.3	5.5 ± 1.8	0.033 ± 0.006	14.9 ± 2.6
GRN7Δtam1Δtam2‡	0.22 ± 0.02	7.1 ± 0.7	20.2 ± 2.6	2.4 ± 0.3	0.029 ± 0.006	13.0 ± 2.6
GRN8Δtam1Δtam2‡	0.17 ± 0.03	5.4 ± 0.9	14.4 ± 6.1	1.7 ± 0.7	0.030 ± 0.006	13.5 ± 2.8
GRN7Δnit1 (BH7)	2.29 ± 0.22	74.5 ± 7.1	488.5 ± 40.0	57.9 ± 4.7	–	–
GRN8Δnit1 (BH13)	1.41 ± 0.29	45.9 ± 9.3	172.4 ± 33.6	20.4 ± 4.0	–	–

Strains were incubated in CM/Glc (starting cell density of 2×10^7/mL) in the presence of 5 mM Trp (*). Strains were incubated in CM/Ara in the presence of 5 mM Trp (†). Concentrations were calculated from peak areas resulting from HPLC analysis. The mean (±SD) values were calculated from three replicates of a single strain (*, †). Two independent strains were investigated and all values averaged (‡).

Ara and in CM/Glc medium (Tables 1 and 2). Thus, Nit1 is not likely to function in a Trp to IAA pathway. To assess further the existence of IAA-related nitrilase activity, we examined whether IAN could serve as substrate for IAA formation in *U. maydis*. As judged from HPLC analysis of culture supernatants of strains FB1 and FB2, detectable IAA was not formed from exogenously applied IAN (0.2 mM) in either CM/Glc or CM/Ara. At higher doses, IAN led to growth reduction, indicative for its uptake (data not shown).

Transaminases are involved in IAA formation from Trp

Tryptophan is efficiently converted to IPA in *U. maydis* strains grown in CM/Glc (Basse *et al.*, 1996), raising the interesting possibility that IPA represents an intermediate in IAA formation from Trp. Formation of IPA requires transaminase activity. The *U. maydis* genome contains two genes, termed *tam1* and *tam2* (MIPS annotation nos. um01804 and um03538; J. Schirawski, in press), encoding predicted aromatic amino acid aminotransferases, with 54% sequence identity to each other, and 25–28% identities to Aro8 and Aro9 of *Saccharomyces cerevisiae*, which function in aromatic amino acid deamination (Iraqui *et al.*, 1998). To assess a contribution of IPA on IAA formation in *Δiad1Δiad2* mutants, *Δiad1Δiad2Δtam1* and *Δiad1Δiad2Δtam1Δtam2* mutant strains were generated (see Experimental procedures). In glucose-containing medium, *Δiad1Δiad2* mutants were only slightly reduced in IAA formation from Trp relative to their wild-type

Table 3 Comparison of pathogenicity symptoms induced by wild-type and IAA mutant strains.

Inoculum	Inoculated plants (*n*)	Symptoms (percentage of inoculated plants)*				
		chl	nod	leaf	stem	total
Series 1 (9 dpi)†						
FB1 × FB2	105	89/85	7/7	25/24	25/24	57/54
BH7 × BH13	107	86/80	3/3	31/29	17/16	51/48
Series 2 (10 dpi)†						
FB1 × FB2	58	56/97	3/5	18/31	24/41	45/78
GRN7 × GRN8	66	64/97	3/5	25/38	21/32	49/74
GRN7Δtam1 × GRN8Δtam1 (#1)‡	62	60/97	3/5	22/35	13/21	38/61
GRN7Δtam1 × GRN8Δtam1 (#2)‡	54	54/100	3/6	18/33	16/30	37/69
Series 3 (6 dpi)†						
FB1 × FB2	36	35/97	0/0	9/25	22/61	31/86
GRN7Δtam1 × GRN8Δtam1	27	26/96	0/0	10/37	14/52	24/89
GRN7Δtam1Δtam2 × GRN8Δtam1Δtam2 (#1)‡	33	33/100	2/6	6/18	24/73	32/97
GRN7Δtam1Δtam2 × GRN8Δtam1Δtam2 (#2)‡	29	29/100	1/3	3/10	22/76	26/90

Symptoms of infected plants: chl, chlorosis only; nod, number of plants with tumours exclusively on nodal shoots; leaf, number of plants with leaf tumours (excluding stem tumours); stem, number of plants with stem tumours (*). Time point (days post inoculation, dpi) of plant inspection (†). Independent combinations of mutant strains (‡). Plants from Series 1 and 3 were used for IAA analysis (see Fig. 6).

strains (Table 2). Interestingly, *Δiad1Δiad2Δtam1* mutants exhibited greater than fivefold reduced IPA and IAA levels relative to *Δiad1Δiad2* mutants, while *Δiad1Δiad2Δtam1Δtam2* mutant strains revealed an additional reduction in the IPA and IAA levels, with IAA levels approximately tenfold reduced relative to *Δiad1Δiad2* mutants (Table 2). The additional effect of the *Δtam2* deletion was only apparent when cells were inoculated at a higher density (Table 2), otherwise *Δtam1* and *Δtam1Δtam2* mutants were similarly reduced (four- to fivefold) in IAA formation from Trp (data not shown). To verify IPA formation from Trp feeding, ethyl acetate-extracted cell-free supernatants were separated by HPLC under two different solvent conditions (see Experimental procedures) and peak fractions were analysed with the Salkowski reagent, which gives a red colour formation with both IAA and IPA (Glickmann and Dessaux, 1995). This revealed that the major peak co-migrating with the IPA standard under acidic conditions shifted to the earlier retention time of IPA under neutral conditions and corresponding peak fractions stained Salkowski-positive, thus corroborating efficient IPA production from Trp (see Supplementary Fig. S1). Together, these results indicate that IPA formation mediated by Tam1 strongly contributes to IAA formation in glucose-containing medium and that Tam2 can support the activity of Tam1.

Next, we investigated whether Tam1 and Tam2 also contribute to IAA formation in medium with arabinose as the carbon source, in which the formation of IPA from Trp is not detected (Basse *et al.*, 1996). Interestingly, *Δiad1Δiad2Δtam1* mutants displayed approximately twofold reduced IAA levels relative to *Δiad1Δiad2* mutants and seven- to eightfold reduced IAA levels relative to wild-type strains, indicating that Tam1 also contributes to IAA formation under these conditions. By contrast, IAA levels were not further lowered in the absence of *tam2* (Table 2). Owing to the absence of detectable IPA formation in CM/Ara, Northern blot analysis was performed to examine whether the *tam1* and *tam2* genes are regulated by the carbon source. This revealed that both genes were expressed in CM irrespective of the carbon source (Fig. 2).

Fungal IAA production and the induction of host tumours

The generated *U. maydis* mutants affected in IAA biosynthesis provided a suitable tool to address the question of whether fungal IAA production is important for tumour induction and the rise of IAA levels in infected host tissue previously reported by Turian and Hamilton (1960). Infection experiments were first performed with *Δiad1Δiad2Δnit1* mutant strains to assess whether these gene deletions have an influence on host IAA levels. The compatible mixture of BH7/BH13 strains (*Δiad1Δiad2Δnit1*) was not affected in the ability to mate and develop dikaryotic hyphae under culture conditions (data not shown). Infection experiments with the host plant maize revealed that tumour formation in the various parts of infected plants was not altered compared with infection with wild-type strains (Table 3).

A time-course experiment was performed to determine IAA levels in response to infection with *Δiad1Δiad2Δnit1* mutants and wild-type strains relative to non-infected plant tissue. For this purpose, a highly sensitive gas chromatography-tandem mass spectrometry technique was applied (Müller *et al.*, 2002). For determination of free IAA levels, extracts were spiked with a

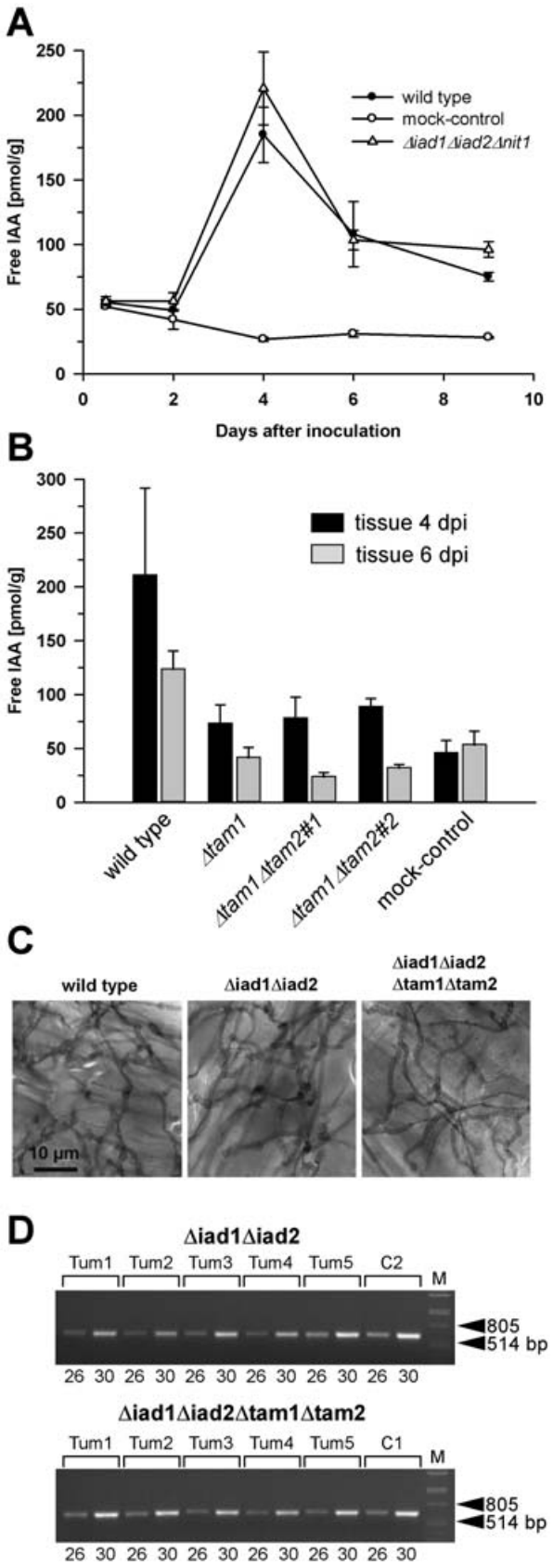

deuterium-labelled internal standard (see Experimental procedures). Although problems with stability of deuterium-labelled IAA standards under alkaline extraction conditions have been reported (Magnus *et al.*, 1980), the applied procedure did not include alkaline hydrolysis, but was based on determination of physiologically active free IAA, and the accuracy of the applied method has been proven. This has shown that the quantities of deuterium-labelled IAA standard recovered from extracts corresponded to the added quantities within limits of experimental error (Müller *et al.*, 2002). In mock-treated plants, IAA levels were between 40 and 50 pmol/g fresh weight within the first 24 h and then declined to values of *c.* 30 pmol/g. In contrast, in wild-type-infected plants, IAA levels rose from 50 to 200 pmol/g 4 days after inoculation and subsequently declined to levels that exceeded those in control tissue by 2.5- to threefold. The IAA profile of plants infected with *Δiad1Δiad2Δnit1* mutants was very similar to that of wild-type-infected plants, with even slightly increased IAA levels (Fig. 6A). Hence, a contribution of Iad1, Iad2 and Nit1 to elevated host IAA levels can be excluded.

Fig. 6 Determination of free IAA levels in maize tissue in response to *U. maydis* infection and analysis of proliferation of *Δiad1Δiad2Δtam1Δtam2* mutants *in planta*. (A) Plants (6 days old) were inoculated with either combinations of FB1/FB2 strains (wild-type; •), BH7/BH13 strains (*Δiad1Δiad2Δnit1*; Δ), or injected with water (mock-control; ❍). (B) Plants were inoculated with either combinations of FB1/FB2 strains (wild-type), FB1Δiad1Δiad2Δtam1/FB2Δiad1Δiad2Δtam1 strains (Δtam1), two independent combinations of FB1Δiad1Δiad2Δtam1Δtam2/FB2Δiad1Δiad2Δtam1Δtam2 strains (Δtam1Δtam2), or injected with water (mock-control). (A,B) Concentrations of IAA are calculated in pmol/g fresh weight. Average values and standard deviations of three data points are given. Leaf material was collected at the time points indicated. For the 12-h and 48-h time points, material was collected 0.5–3 cm above ground and 0.5–3 cm below the injection site, respectively. For the 4-, 6- and 9-day time points, chlorotic or early leaf tumour (4 days) and leaf tumour (6 and 9 days) tissue was collected between the ligule and > 1 cm below the injection site. All parts were exclusively from the third and fourth leaves. Non-infected control material was isolated correspondingly. For each time point, ten or more tissue samples were collected. (C) Maize plants were inoculated with either mixtures of FB1/FB2 (wild-type), FB1Δiad1Δiad2/FB2Δiad1Δiad2 (Δiad1Δiad2) or FB1Δiad1Δiad2Δtam1Δtam2/FB2Δiad1Δiad2Δtam1Δtam2 (Δiad1Δiad2Δtam1Δtam2) strains. Two days after inoculation samples from infected leaf blade tissue were stained with Chlorazol Black E. Note the ramification of hyphae throughout the epidermal layer. The bar (10 µm) refers to all panels. (D) Detection of FB1Δiad1Δiad2/FB2Δiad1Δiad2 (Δiad1Δiad2) and FB1Δiad1Δiad2Δtam1Δtam2/FB2Δiad1Δiad2Δtam1Δtam2 (Δiad1Δiad2Δtam1Δtam2) strain combinations in maize tumours. Chromosomal DNA (100 ng) isolated from each of five individual tumours (Tum1–5) 6 days after inoculation with either of these combinations was used as template for PCR to amplify a fungal-specific DNA fragment (see Experimental procedures). C1, C2: DNA (100 ng) isolated from the respective strain combinations prior to plant infection was used as template. Twenty-six and 30 cycles (numbers below the lanes) were performed. The expected size of the amplified fragment is 633 bp. All lanes are from the same gel. Phage lambda (M) DNA (500 ng) digested with *Pst*I was used as size marker.

Next, plant infection experiments were performed with the *Δiad1Δiad2Δtam1* and *Δiad1Δiad2Δtam1Δtam2* mutant strains, which are severely reduced in IAA formation in both CM/Ara and CM/Glc. Compatible mixtures of these mutants were not affected in their ability to mate and develop dikaryotic hyphae (data not shown). Inspection of infected plants revealed that these mutants triggered disease symptoms comparable with wild-type strains (Table 3). However, host tissue harvested 4 days after inoculation with compatible mixtures of either *Δiad1Δiad2Δtam1* or *Δiad1Δiad2Δtam1Δtam2* mutant strains contained significantly lower IAA amounts than comparable tissue of wild-type-infected plants (Fig. 6B). This difference persisted in tumour tissue harvested 6 days after inoculation. Here, IAA levels in tissue infected with mutant strains were slightly below the IAA levels in mock-treated control tissue, whereas tissue from wild-type-infected plants showed a 2.5- to threefold increase (Fig. 6B). In conclusion, this implies that fungal IAA derived from IPA critically contributes to host IAA levels. However, fungal IAA production is apparently not important for induction of host tumours.

Furthermore, we assessed whether identified *U. maydis* genes involved in IAA formation contributed to fitness during plant infection. Infected leaf blade sections were collected 2, 4 and 6 days after inoculation with either wild-type, *Δiad1Δiad2* or *Δiad1Δiad2Δtam1Δtam2* strain combinations for microscopic analysis. This showed extensive hyphal proliferation throughout epidermal cells and in underlying tissue already at the 2-day time point for all strain combinations (Fig. 6C and data not shown). In addition, no apparent differences in hyphal ramification between these combinations were detected at later stages (data not shown). Fungal proliferation in individual tumours 6 days after inoculation with the *Δiad1Δiad2* and the *Δiad1Δiad2Δtam1Δtam2* strain combinations, respectively, was further assessed by PCR analysis. This revealed that the *Δiad1Δiad2Δtam1Δtam2* strain combination was able to proliferate at the same rate as the parental *Δiad1Δiad2* combination (Fig. 6D), indicating that the reduced IAA amounts in host tissue infected with the quadruple mutants were not the result of impaired fungal proliferation.

DISCUSSION

Recapitulation of IAA biosynthesis in *U. maydis* has revealed that indole-3-acetaldehyde dehydrogenase activities of Iad1 and Iad2 are central for the conversion of both IAAld and TAM to IAA and has emphasized a connection between IPA and IAA formation. The route of IAA formation from Trp depends strongly on the carbon source. While IAA formation via IPA predominates in glucose-containing medium independently of Iad1 and Iad2, IAAld dehydrogenase-mediated IAA formation proceeds in the absence of glucose. *U. maydis* mutants blocked in IPA formation and devoid of IAAld dehydrogenase activity were most severely affected in the conversion of Trp to IAA and gave insight into the contribution of fungal IAA formation to elevated IAA levels in infected host tissue and induction of host tumours.

Indole-3-acetaldehyde dehydrogenases in *U. maydis*

We have identified the *iad2* gene encoding an IAAld dehydrogenase, responsible for the residual IAA formation from IAAld in *Δiad1* mutants. However, the contributions of Iad1 and Iad2 to IAA formation are not equal and, in contrast to *Δiad1* mutants, *Δiad2* mutants are not significantly reduced in IAA formation from IAAld. The severe loss of IAAld dehydrogenase activity in *ΔiadΔ1iad2* mutants suggests a concerted action of both enzymes and excludes redundant enzyme activities among the additional predicted aldehyde dehydrogenases in *U. maydis*. Of note, the ability to function as IAAld dehydrogenase does not correlate with sequence similarity to Iad1 as exemplified from the finding that Pad2, which exhibits the highest similarity to Iad1, lacks IAAld dehydrogenase activity. Conceivably, amino acids specific for Iad1 and Iad2 participate in substrate specificity. An alignment of the Iad1 and Iad2 sequences revealed C-terminally localized amino acids exclusively shared between Iad1 and Iad2 and not found in any of the other predicted aldehyde dehydrogenase sequences in *U. maydis* (see Fig. 3; data not shown). Thus, it will be tempting to explore whether these residues in Iad1 and Iad2 play a role in substrate recognition.

IAA formation via a possible tryptamine pathway in *U. maydis*

The requirement for both Iad1 and Iad2 to convert TAM to IAA together with the significant contribution of Iad1 to IAA formation from Trp in CM/Ara provides evidence for a TAM pathway in *U. maydis*. However, it is presently unclear how TAM is converted to IAAld and whether IAOx is involved in IAA formation. HPLC analysis of cell-free cultures from Trp as well as from TAM feeding experiments in CM/Ara did not reveal a compound eluting like IAOx (data not shown), leaving the possibility that IAOx is rapidly metabolized. Due to the prevalent role of Iad1 in IAA biosynthesis from TAM, the inability for TAM to IAA conversion in the presence of glucose cannot be attributed to the lack of Iad2 activity, but indicates that additional enzymes acting downstream of TAM must be under glucose repression. In Arabidopsis, the YUCCA enzyme is able to convert TAM to *N*-hydroxyl-TAM and members of the Arabidopsis *YUC* gene family play a key role in auxin biosynthesis and plant development (Cheng *et al.*, 2006; Zhao *et al.*, 2001). However, enzymes acting downstream of YUCCA remain elusive. In this respect, the *U. maydis* cell culture system based on precursor feeding could provide a means by which mutants blocked in TAM conversion can be identified and the responsible genes cloned.

The role of indole-3-pyruvic acid in IAA formation in *U. maydis*

In glucose-containing medium, *U. maydis* efficiently produces IPA from Trp (Basse *et al.*, 1996). We now implicate the *tam1* and *tam2* genes encoding potential aromatic amino acid aminotransferases in this pathway. The absence of *tam1* strongly reduced IPA formation from Trp and caused a marked decrease in IAA levels, emphasizing that IPA serves as an efficient precursor for IAA formation from Trp in *U. maydis*. Levels of IPA and IAA could be further diminished in the absence of *tam2*, indicating that both Tam1 and Tam2 function as Trp aminotransferase. The restriction of detectable IPA formation to glucose-containing medium was not reflected at the transcriptional level of *tam1* and *tam2*, suggesting regulation at the post-transcriptional level. Furthermore, the observation that *tam1* also contributed to IAA formation from Trp in medium with arabinose as the carbon source implies low levels of IPA accumulation also under these conditions. In *S. cerevisiae*, Aro8 and Aro9 function in Trp deamination. Aro8 expression is subject to the general control of amino acid biosynthesis (Iraqui *et al.*, 1998). While the catabolic enzyme Aro9 is mainly involved in Trp degradation, Aro8 aminotransferase is responsible for Phe and Tyr biosynthesis (Iraqui *et al.*, 1998 and references therein). Future investigations need to show whether such distinct roles can also be ascribed to *U. maydis tam1* and *tam2* products.

In contrast to *Δtam1* mutants, the *Δiad1Δiad2* mutants were only weakly reduced in IAA formation from Trp in glucose-containing medium. As IAAld dehydrogenase activity is central within the IPA pathway, this implies that a major portion of IPA is not metabolized to IAA via IAAld, but probably via non-enzymatic degradation due to the unstable nature of IPA in aqueous solutions (Sheldrake, 1973).

The observation of residual IAA formation in *Δiad1Δiad2Δtam1Δtam2* mutants points to additional intermediates besides IPA and IAAld in the conversion of Trp to IAA. However, we could not provide evidence for IAA formation from IAN in *U. maydis* and the predicted nitrilase Nit1 does not contribute to IAA formation. With respect to the bacterial IAM pathway known from plant pathogenic bacteria, the *U. maydis* genome annotated by MIPS contains no sequence with significant similarity to bacterial Trp 2-monooxygenases. By contrast, the *U. maydis* genome revealed two predicted amidase genes (MIPS annotation nos. um10207 and um04505), whose deduced amino acid sequences show strong similarity (> 35% identity) to the highly conserved stretch of 118 amino acids of *Agrobacterium tumefaciens* IAM hydrolase (accession no. P25016), which includes the catalytic site residues (Kobayashi *et al.*, 1997; Pollmann *et al.*, 2003). Feeding experiments of *U. maydis* cultures with IAM revealed IAA formation, although a > 50-fold elevated substrate concentration was required to yield similar IAA amounts as produced from 20 μm IAAld (C. W. Basse, unpublished data).

IAA formation in other fungal species

In contrast to the broad insight into IAA biosynthesis pathways in plants and bacteria (Spaepen *et al.*, 2007), little is known about IAA biosynthesis in fungi. Possible intermediates reported thus far are IAAld, IPA, TAM and IAM (see Fig. 1), suggesting the occurrence of the IPA, TAM and IAM pathways, respectively, while consistent with our study, IAA formation via IAN has not been reported (Chung and Tzeng, 2004 and references therein). Pathways involving IAAld and IAM were reported for the phytopathogenic fungi *Colletotrichum gloeosporioides* f.sp. *aeschynomene* and *Colletotrichum acutatum* (Chung *et al.*, 2003; Robinson *et al.*, 1998). In *C. gloeosporioides*, feeding with IAM resulted in efficient IAA formation, while IAAld was mainly converted to Tol with minor IAA formation (Robinson *et al.*, 1998). In both species, IAM accumulated as an intermediate from Trp feeding, although no or only low amounts of IPA were detected in culture filtrates. This indicates marked differences to *U. maydis*, in which efficient conversion of Trp to IPA and of IAAld to IAA occurs. The ability to synthesize IAA from Trp was also detected in *Ustilago esculenta* and *U. scitaminea*. Reminiscent of *U. maydis*, *U. esculenta* converted IAAld to IAA efficiently; however, IAM did not serve as a precursor compound (Chung and Tzeng, 2004). Increased amounts of IAA were also measured in galls of the aquatic grass *Zizania latifolia* in response to infection with *U. esculenta* (Chung and Tzeng, 2004) and in citrus flower petals infected with *C. acutatum* causing post-bloom fruit drop (Lahey *et al.*, 2004). While these studies demonstrate fungal IAA production from Trp and suggest underlying pathways, the responsible genes have not been identified and hence a possible influence of fungal IAA formation on the development of disease symptoms could not be addressed in these systems.

Role of fungal IAA in tumour formation

The generation of *U. maydis* mutants severely compromised in IAA formation allowed us to address a possible role of fungal IAA production in host tumour formation. Turian and Hamilton (1960) demonstrated 20- and fivefold higher IAA concentrations in tumour tissue prior to and during sporulation, respectively, compared with non-infected maize stalk tissue. We now show that free IAA levels increase only transiently in leaves prior to sporulation. Their determination of an IAA concentration of 24 nM in non-infected tissue is similar to the IAA concentration of 25–50 nM in non-infected leaf tissue as reported here, with a culmination of free IAA amounts in infected leaf tissue at the 4-day time point, which coincides with the onset of visible tumour formation. IAA is the major auxin in plants and has profound roles in the regulation of plant growth and development, including cell division, elongation and differentiation (Estelle, 1992; Friml, 2003; Kepinski and Leyser, 2003). Thus, IAA might also play

a role in increased cell growth associated with tumour formation after *U. maydis* infection (Callow and Ling, 1973; Doehlemann *et al*, 2007; Snetselaar and Mims, 1994). Among the generated *U. maydis* mutant strains, those harbouring the *Δtam1* deletion were most severely affected in IAA formation in culture. Surprisingly, none of the triple or quadruple mutants constructed was affected in triggering tumour formation on different organs of infected plants. However, in 6-day-old tumour tissue from plants infected with these mutant strains, IAA levels were no longer increased over those in non-infected tissue (see Fig. 6B). This indicates that the fungal conversion of Trp to IPA critically contributes to IAA levels in *U. maydis*-infected tissue, but this is not essential for host tumour formation. The finding that IAA levels are still increased about twofold when mock-infected tissue and tissue infected with the *Δiad1Δiad2Δtam1* mutants are compared at the 4-day time point (see Fig. 6B) suggests that this increase results either from increased synthesis by the host (Kriechbaumer *et al*., 2006) or from mobilization of auxin from conjugates (Woodward and Bartel, 2005). The maize *ZmNit2* gene has been proposed to participate in IAA formation in maize kernels (Park *et al*., 2003). Northern blot analysis of *zmnit2* transcript levels in *U. maydis*-infected leaf tissue from immediately to 6 days after inoculation indicated constitutive expression, thus providing no clue for induced IAA biosynthesis during tumour formation (B. Heinze and C. Basse, unpublished data). In support of a role of IAA in host tumour formation, DNA-array analysis has revealed strong upregulation of the maize expansin genes *EXPA4*, *EXPB3* and *EXPB8* (NCBI accession nos. AY106266.1, BM381516 and AA072435) in 5-day-old tumour tissue (var. Early Golden Bantam) infected with strains FB1 and FB2 compared with mock-infected tissue (M. Vranes and J. Kämper, unpublished data). Expansins induce cell expansion and their induced expression depends on polar auxin transport (Tanaka *et al*., 2006). Several reports have highlighted the ability of plant-colonizing bacteria to modulate auxin signalling in plants and provided examples for interference of auxins with the host defence system (Spaepen *et al*., 2007). In *U. maydis*-infected maize tissue, signs of a weak defence response, such as production of the antimicrobial compound DIMBOA, and *PR-1* gene expression have been observed (Basse, 2005). The *U. maydis* IAA mutant strains generated may now be exploited to assess an influence of fungal IAA on defence- as well as tumour-related host gene expression.

EXPERIMENTAL PROCEDURES

Strains, growth conditions and chemicals

Escherichia coli K12 strain TOP10 (Invitrogen, Karlsruhe, Germany) was used as host for plasmid amplification. *Ustilago maydis* strains FB1 (*a1b1*), FB2 (*a2b2*), FB1Δiad1, FB2Δiad1 and 521 (*a1b1*) have been described previously (Banuett and Herskowitz, 1989; Basse *et al*., 1996; Kämper *et al*., 2006). The antibiotics carboxin (cbx), nourseothricin (nat) and phleomycin (ble) used for *U. maydis* selection were purchased from Riedel-de Haën (Hannover, Germany), Werner BioAgents (Jena-Cospeda, Germany) and Invivogen (Toulouse, France), respectively. *U. maydis* strains were grown at 28 °C in YEPSL medium [1% (w/v) yeast extract, 0.4% (w/v) peptone, 0.4% (w/v) sucrose] modified from Tsukuda *et al*. (1988) or complete medium (CM) (Holliday, 1974). Mating of compatible strains was performed on solid charcoal-containing CM at room temperature for 48 h (Holliday, 1974). Infection of 6-day-old maize (*Zea mays*) plants (var. Early Golden Bantam; Olds Seed, Madison, WI) was performed as described (Basse, 2005). Sporidia were adjusted to cell densities of about 4×10^7/mL prior to inoculation. HPLC solvents and water were from Mallinckrodt Baker (Griesheim, Germany). All other chemicals were of analytical grade and obtained from Sigma (Taufkirchen, Germany) or Roth (Karlsruhe, Germany).

DNA and RNA procedures

DNA and RNA procedures were performed as described (Basse *et al*., 2000). ^{32}P-labelled fragments for DNA and RNA gel blot analysis were generated using the NEBlot kit (New England Biolabs, Frankfurt am Main, Germany). Detection and quantification of radioactive signals was done using a STORM PhosphorImager and ImageQuant software (Molecular Dynamics, Sunnyvale, CA). For Southern blot analysis, genomic DNA from strain FB1Δiad1 was digested with *Pst*I and probed with the ^{32}P-labelled *Age*I/*Bst*BI *iad1* fragment (Basse *et al*., 1996). Southern hybridization was performed under non-stringent conditions at 60 °C omitting stringent washing steps. For RNA gel blot analysis, probes for *iad2* (positions 231–1446 of um03402), *tam1* (28–1129 of um01804) and *tam2* (289–1454 of um03538) were amplified from genomic DNA (strain FB1). The *pad16* probe was isolated as *Nco*I/*Xho*I fragment from pBADpad16 (see below). The *ppi* probe has been described (Bohlmann, 1996). PCR-based isolation of *iad2* was performed with genomic FB1Δiad1 DNA and the degenerate oligonucleotides AD22 (5′-GGAATTCAARAARGTBACNCTBGAR-3′; IUPAC-code; restriction site underlined) and AD44 (5′-GGAATTCTTRWADCCDCCRAANGG-3′) deduced from the amino acid sequences KKVTLE (AD33) and PFGG$^{Y}/_{F}$K (AD44), respectively, conserved among Iad1 and a number of fungal aldehyde dehydrogenase sequences (accession nos. A39410, P42041, P41751 and P40108). Southern blot analysis of cloned PCR fragments was performed to identify DNA fragments different from *pad2* and *pad3*.

Constructs for expression in *E. coli*

For expression in pBAD102/D-TOPO (Invitrogen) the entire ORFs of selected genes were amplified from genomic DNA of strain 521 (PfuUltra, Stratagene, Amsterdam, The Netherlands) using the

following primer pairs: 5′-CACCATGGCAACTCTCAACCTCGATCTG-3′/5′-GATAGGGGCAGGCTGGCTGAGGTTC-3′ (*iad1*); 5′-CACCATGGACTCATCGCATGGTACAAC-3′/5′-CAGTTTGGGAAGCGGCCA-ATCG-3′ (*pad2*); 5′-CACCATGGCTGTTGGCGTTGCTTC-3′/5′-GGC-TTTGGGGATCCAGAGTGCTTG-3′ (*iad2*); 5′-CACCATGGCTGAAC-CCGTCTGCACG-3′/5′-AGCGTCAAACACGACACCCTGC-3′ (*pad16*). PCR products were cloned into the pBAD102/D-TOPO vector. The *thx* region at the 5′ positions of the inserted ORFs was removed by deleting the smaller internal *Nco*I fragment. Final plasmids were denoted pBADiad1, pBADpad2, pBADiad2, and pBADpad16, respectively.

Deletion of *iad2*

A 3273-bp genomic *Hind*III fragment comprising the complete *iad2* ORF between positions 452 and 1900 was isolated from a cosmid library (Bölker *et al*., 1995) and cloned into pUC18 (Amersham-Pharmacia Biotech, Freiburg, Germany) to yield plasmid pCIII. An internal *Pml*I fragment (positions 661–1930) was replaced with the nat resistance cassette isolated as *Not*I(blunt) fragment from plasmids pSLNat (Müller *et al*., 2003). The resulting plasmid pCIIInatVI was linearized at the *Aat*II site prior to transformation into *U. maydis* strains FB1, FB2, FB1Δiad1 and FB2Δiad1. Demonstration of homologous integration was based on PCR using a primer pair within the deleted region and primer combinations spanning flanking regions between the resistance cassette and positions beyond the *Hind*III site on either side.

Deletion of *nit1*, *tam1* and *tam2*

Δnit1, *Δtam1* and *Δtam2* deletion strains were generated applying the PCR-based protocol (Kämper, 2004). Flanking sequences of *c*. 1 kb were amplified (Phusion™ High-Fidelity PCR, New England Biolabs) from chromosomal DNA of *U. maydis* strains FB1 (*Δtam1*, *Δnit1*) and 521 (*Δtam2*). Primer combinations used were: 5′-GGGTATTTGATCAGCTCTTGATCC-3′/5′-GTGGGCCATC-TAGGCCTGTTGTTGCCGTGAGAGGTGC-3′ (left flank of *nit1*) and 5′-CACGGCCTGAGTGGCCGAAAGCGCCGAGCGTGACAAGG-3′/5′-GCTCAAAGTCTTCAGAGCGGAGCA-3′ (right flank of *nit1*), 5′-GCTCGTCTGGGGTACCATGCAAG-3′/5′-CACGGCCTGAGTGG-CCTGGCGATGTGGCCGAGGACATC-3′ (left flank of *tam2*) and 5′-GTGGGCCATCTAGGCCGGCTCCAGATTCCTGCCTAG-3′/5′-CA-TGTCAACAGACCCAGCTGC-3′ (right flank of *tam2*), 5′-ATAATG-GCCACGTGGGCCAGCCGCAAAGTCGAATAAGC-3′/5′-ATAATGG-CCTGAGTGGCCGGTTTGACAGGGAGGATATTGG-3′ (left flank of *tam1*) and 5′-ATCTAGGCCATCTAGGCCTGAGCTCGCTTAAATGG-3′/5′-ATAATGGCCACGTGGGCCGATTCATACTCGCGGAACC-3′ (right flank of *tam1*). PCR products were cleaved with *Sfi*I (recognition sites underlined in primers) for ligation with the ble (*Δtam2*) or cbx (*Δnit1*, *Δtam1*) resistance cassettes isolated with *Sfi*I from pMF1-p and pMF1-c, respectively (Brachmann *et al*., 2004). Ligation products were cloned into the pCR2.1, pCR4-TOPO or pCR4Blunt-TOPO vectors (Invitrogen), from which they were re-amplified or isolated for subsequent transformation in *U. maydis*. Homologous integration of all constructs was analysed by PCR using a primer pair within the deleted region and primer combinations spanning flanking regions on either side, as described (Kämper, 2004). For additional Southern blot analysis of *Δnit1*, *Δtam1* and *Δtam2* deletion strains, genomic DNA was restricted with *Nde*I, *Bam*HI and *Bss*HII, respectively, and probed with either the left flank of the deletion construct (*Δnit1*) or the entire deletion constructs (*Δtam1*, *Δtam2*).

Growth conditions of *E. coli* and enzyme assays

E. coli strains harbouring pBAD102/D-TOPO constructs were incubated in Luria–Bertani medium containing ampicillin (100 μg/mL) at 37 °C under shaking. Arabinose was added to a final concentration of 0.1% (w/v) to cultures at an A_{600} of 0.5 and incubation was continued for 5 h (t_1) under the same conditions. Control incubations occurred in the absence of arabinose. Pellets from 50 mL of culture were harvested at t_1, resuspended in ice-cold enzyme extraction buffer (50 mM Tris-HCl, pH 7.5; 5 mM dithiothreitol, 0.2 mM EDTA, Complete Protease Inhibitor; Roche, Mannheim, Germany) and stored frozen at –80 °C. Cells were thawed and disrupted in a chilled (0 °C) French pressure cell (SLM-Aminco Instruments, IL). Cell lysates were centrifuged (15 min, 10 000 ***g***, 4 °C) and supernatants desalted on a PD-10 column (Amersham-Pharmacia Biotech) as described (Basse *et al*., 1996). Protein concentrations were determined according to the Bradford method using bovine serum albumin as standard. Protein preparations (50 μL corresponding to 0.7 mL of cell culture) were incubated in the presence of 0.5 mM IAAld in 200 μL 60 mM Tris-HCl, pH 7.0, 100 mM KCl, 1 mM NAD^+ for 30 min at 30 °C. Reaction mixtures were acidified with HCl, extracted with ethyl acetate, which removes IAAld, and analysed for IAA formation with the use of the Salkowski reagent or by reversed-phase HPLC (gradient II) as described (Basse *et al*., 1996; see below).

HPLC analysis

HPLC analysis was performed on Beckman Coulter (Krefeld, Germany) System Gold 126/168 solvent/detector modules equipped with a C18 ultrasphere column (4.6 × 250 mm) connected to a precolumn (4.6 × 45 mm) (both 5 μm; Beckman Coulter). Solvent conditions were as described (Basse *et al*., 1996). Gradient I (based on 0.1% trifluoroacetic acid) was run to separate extracts from Trp feeding and gradient II (based on 20 mM ammonium acetate, pH 6.5) was run to separate extracts from IAAld and TAM feedings. The identity of IAA formation from Trp has previously been verified by mass spectroscopy (Basse *et al*., 1996). The strong

shifts in the retention time values for IAA and IPA between gradients I and II (see supplementary Fig. S1) are due to the negative charge of the carboxyl group under neutral conditions. Peak areas were calculated using the 32 Karat Software tool (Beckman Coulter). Collected fractions were dried under vacuum for the detection of IAA or IPA with the Salkowski reagent. Water treated with the Salkowski reagent served as blank. Colorimetric reactions were measured with a SAFIRE microplate reader (TECAN, Grödig, Austria) at 530 nm.

Immunoblot analysis

Frozen *E. coli* cell pellets collected at t_1 (see above) were thawed and boiled in Laemmli buffer, and protein amounts (corresponding to 40 μL of cell culture) were applied to sodium dodecyl sulphate (SDS)-PAGE (10%) for subsequent immunoblot analysis using an anti-His (C-term) antibody (1 : 5000 dilution of a 1.01 mg/mL solution; Invitrogen). A goat anti-mouse IgG-horseradish peroxidase conjugate (1 : 2500 diluted; Promega, Mannheim, Germany) was used as secondary antibody. The Broad Range prestained protein marker from New England Biolabs was used as size marker (10 μL per lane).

Feeding experiments

U. maydis was cultivated with either tryptophan (5 mM), IAAld (20 μM or 0.2 mM) or tryptamine (0.5 mM) in CM/Ara (1%, w/v) or CM/Glc (1%, w/v). Cultures started at cell densities of *c.* 2×10^6/mL, if not otherwise indicated, and were incubated under shaking (200 r.p.m.) at 28 °C for 14 h. Cell-free supernatants were analysed with the Salkowski reagent and by reversed-phase HPLC (gradients I and II) as described (Basse *et al.*, 1996). Strain FB1 cultivated in the respective CM medium in the absence of the supplemented precursor, and non-inoculated medium containing the precursor served as blank values for product quantification from optical densities at 220 nm. Strains were inoculated in parallel for triplicate measurements.

Determination of IAA in plant tissue

Plant tissue (pooled from ten or more samples collected from different plants each) was harvested and immediately frozen in liquid nitrogen. For IAA determination, tissue was ground in liquid nitrogen and resuspended in methanol to a concentration of 0.25 g plant material (fresh weight)/mL. Three samples (replicates) of 1 mL each (0.25 g fresh plant material per sample) were removed, supplemented with 25 pmol $[^2H]_2$-IAA (internal standard; Campro Scientific, Berlin, Germany) and incubated under shaking for 3 min at 50 °C. Incubation was continued for 10 min under shaking at 25 °C and without shaking for 1 h at 25 °C. Cell-free supernatants were removed, the pellets were washed with 0.5 mL methanol and the combined supernatants were dried under vacuum for subsequent gas chromatography-tandem mass spectrometry analysis as previously described (Müller *et al.*, 2002). In brief, the dried residues were dissolved in 30 μL methanol, to which 200 μL diethyl ether was added, followed by ultrasonic treatment (Sonorex RK510S; Bandelin, Berlin, Germany). The particle-free sample was then applied to a custom-made microscale aminopropyl solid-phase extraction-cartridge. The cartridge was washed with 250 μL $CHCl_3$:2-propanol = 2:1 (v/v), and the hormone-containing fraction thereafter eluted with 400 μL acidified diethyl ether (2% acetic acid, v/v). The eluates were taken to dryness, re-dissolved in 20 μL methanol, and afterwards treated with 100 μL ethereal diazomethane and transferred to autosampler vials [Chromacol 05-CTV(A) 116; Fisher Scientific, Schwerte, Germany]. Excessive diazomethane and remaining solvent were removed in a gentle stream of nitrogen, and the methylated samples were then taken up in 15 μL of chloroform. To analyse the contents of acidic phytohormones in the samples, an aliquot of 1 μL of each was injected into the GC-MS system. All spectra were recorded on a Varian Saturn 2000 ion-trap mass spectrometer connected to a Varian CP-3800 gas chromatograph (Varian, Walnut Creek, CA), equipped with a ZB-50 fused silica capillary column (Phenomenex, Torrance, CA). The mass spectrometer was used in CI-MRM mode with methanol as the reactant gas and positive ion detection. The setting for endogenous IAA was chosen as follows: IAA $m/z = 190$ $[M + H]^+$, 0.50 V. A second channel analysing the $[^2H]_2$-IAA standard used an identical excitation amplitude for the following parent ion: $[^2H]_2$-IAA $m/z = 192$ $[M + H]^+$. The amount of endogenous compound was calculated from the signal ratio of the unlabelled over the stable isotope-containing mass fragment observed in both analysing channels.

Detection of *U. maydis* in infected maize tissue

Infected leaf blade tissue was collected exclusively from the third and fourth leaves beneath the inoculation site. Staining with Chlorazol Black E (CBE) followed the method of Brundrett *et al.* (1996). Chromosomal DNA from infected maize tissue was isolated with the DNeasy plant kit (Qiagen, Hildesheim, Germany). Detection of fungal DNA in infected plant tissue was performed by PCR analysis using the combination of 5′-GACCACTCTTGACGACACG-GCTTACC-3′/5′- GGCGTGAATGTAAGCGTGACATAAC-3′ primers, which specifically bind within the nat resistance cassette. The absence of *tam1* (um01804) in strain combinations carrying the *Δtam1* deletion was ensured by using the combination of 5′-TGAGAGCCTCTCGCTGAACCTCAAGC-3′/5′-GGATCTTGGA-GAAGCTCTCGAAACG-3′ *tam1*-specific primers.

Databases

Nucleotide sequences were compared using the NCBI database with BLAST, and accession numbers refer to this database if

not otherwise indicated. Genomic sequences of *U. maydis* were retrieved from the Broad Institute (http://www.broad.mit.edu/annotation/fungi/ustilago_maydis/). Protein sequences and um numbers were retrieved from the MIPS (Munich Information Center for Protein Sequences) *Ustilago maydis* Database (MUMDB; http://mips.gsf.de/genre/proj/ustilago/). Predictions of mitochondrial targeting sequences were made with MITOPROT (http://www.expasy.ch).

ACKNOWLEDGEMENTS

We thank the Deutsche Forschungsgemeinschaft for financial support of B.H. (grant no. SFB 395). We are grateful to Professor Elmar Weiler and his technical assistant Petra Düchting, Ruhr-University of Bochum, Germany, for their generous support in the determination of IAA levels in maize tissue and for providing the IAOx standard. We thank Stephan Stumpferl for the isolation of *U. maydis pad2*, *pad3* and *iad2* fragments, Kai Luh and Emine Kaya for their support in generating *Δtam2* mutants, Katja Zuther for providing the *Δtam1* deletion construct, and Kathrin Auffarth and Elmar Meyer for technical assistance. In addition, we would like to thank Dr Stephan Pollmann (Ruhr-University of Bochum) for providing detailed information to the GC-MS protocol for IAA analysis.

NOTE ADDED IN PROOF

The citation J. Schirawski, unpublished data, has now been published: The tryptophan aminotransferase Tam1 catalyses the single biosynthetic step for tryptophan-dependent pigment synthesis in *Ustilago maydis*. Zuther, K., Mayser, P., Hettwer, U., Wu, W., Spiteller, P., Kindler, B.L.J., Karlovsky, P., Basse, C.W. and Schirawski J. Molecular Microbiology Published article online: 26-Feb-2008 doi: 10.1111/j.1365-2958.2008.06144.x.

REFERENCES

Bak, S., Tax, F.E., Feldmann, K.A., Galbraith, D.W. and Feyereisen, R. (2001) CYP83B1, a cytochrome P450 at the metabolic branch point in auxin and indole glucosinolate biosynthesis in Arabidopsis. *Plant Cell*, **13**, 101–111.

Banuett, F. and Herskowitz, I. (1989) Different *a* alleles of *Ustilago maydis* are necessary for maintenance of filamentous growth but not for meiosis. *Proc. Natl Acad. Sci. USA*, **86**, 5878–5882.

Banuett, F. and Herskowitz, I. (1996) Discrete developmental stages during teliospore formation in the corn smut fungus, *Ustilago maydis*. *Development*, **122**, 2965–2976.

Barlier, I., Kowalczyk, M., Marchant, A., Ljung, K., Bhalerao, R., Bennett, M., Sandberg, G. and Bellini, C. (2000) The *SUR2* gene of *Arabidopsis thaliana* encodes the cytochrome P450 CYP83B1, a modulator of auxin homeostasis. *Proc. Natl Acad. Sci. USA*, **97**, 14819–14824.

Basse, C.W. (2005) Dissecting defense-related and developmental transcriptional responses of maize during *Ustilago maydis* infection and subsequent tumor formation. *Plant Physiol.* **138**, 1774–1784.

Basse, C.W. and Steinberg, G. (2004) Pathogen profile: *Ustilago maydis*, model system for analysis of the molecular basis of fungal pathogenicity. *Mol. Plant Pathol.* **5**, 83–92.

Basse, C.W., Lottspeich, F., Steglich, W. and Kahmann, R. (1996) Two potential indole-3-acetaldehyde dehydrogenases in the phytopathogenic fungus *Ustilago maydis*. *Eur. J. Biochem.* **242**, 648–656.

Basse, C.W., Stumpferl, S. and Kahmann, R. (2000) Characterization of a *Ustilago maydis* gene specifically induced during the biotrophic phase: evidence for negative as well as positive regulation. *Mol. Cell. Biol.* **20**, 329–339.

Bohlmann, R. (1996) *Isolierung und Charakterisierung von filamentspezifisch exprimierten Genen aus Ustilago maydis*. PhD thesis, LMU Munich.

Bölker, M., Böhnert, H.U., Braun, K.-H., Görl, J. and Kahmann, R. (1995) Tagging pathogenicity genes in *Ustilago maydis* by restriction enzyme-mediated integration (REMI). *Mol. Gen. Genet.* **248**, 547–552.

Brachmann, A., König, J., Julius, C. and Feldbrügge, M. (2004) A reverse genetic approach for generating gene replacement mutants in *Ustilago maydis*. *Mol. Genet. Genomics*, **272**, 216–226.

Brundrett, M., Bougher, N., Dell, B., Grove, T. and Malajczuk, N. (1996) *Working with Mycorrhizas in Forestry and Agriculture, Monograph 32*. Canberra, Australia: Australian Centre for International Agricultural Research.

Callow, J.A. and Ling, I.T. (1973) Histology of neoplasms and chlorotic lesions in maize seedlings following the injection of sporidia of *Ustilago maydis* (DC) Corda. *Physiol. Plant Pathol.* **3**, 489–494.

Cheng, Y., Dai, X. and Zhao, Y. (2006) Auxin biosynthesis by the YUCCA flavin monooxygenases controls the formation of floral organs and vascular tissues in *Arabidopsis*. *Genes Dev.* **20**, 1790–1799.

Christensen, J.J. (1963) *Corn smut caused by Ustilago maydis*. St. Paul, MN: American Phytopathological Society.

Chung, K.R. and Tzeng, D.D. (2004) Biosynthesis of indole-3-acetic acid by the gall-inducing fungus *Ustilago esculenta*. *J. Biol. Sci.* **4**, 744–750.

Chung, K.R., Shilts, T., Erturk, U., Timmer, L.W. and Ueng, P.P. (2003) Indole derivatives produced by the fungus *Colletotrichum acutatum* causing lime anthracnose and postbloom fruit drop of citrus. *FEMS Microbiol. Lett.* **226**, 23–30.

Cooney, T.P. and Nonhebel, H.M. (1989) The measurement and mass spectral identification of indole-3-pyruvate from tomato shoots. *Biochem. Biophys. Res. Commun.* **162**, 761–766.

Doehlemann, G., Wahl, R., Vranes, M., de Vries, R.P., Kämper, J. and Kahmann, R. (2007) Establishment of compatibility in the Ustilago maydis/maize pathosystem. *J. Plant. Physiol.* **165**, 29–40.

Estelle, M. (1992) The plant hormone auxin: insight in sight. *Bioessays*, **14**, 439–444.

Fedorova, E., Redondo, F.J., Koshiba, T., Pueyo, J.J., de Felipe, M.R. and Lucas, M.M. (2005) Aldehyde oxidase (AO) in the root nodules of *Lupinus albus* and *Medicago truncatula*: identification of AO in meristematic and infection zones. *Mol. Plant–Microbe Interact.* **18**, 405–413.

Friml, J. (2003) Auxin transport-shaping the plant. *Curr. Opin. Plant Biol.* **6**, 7–12.

Glickmann, E. and Dessaux, Y. (1995) Critical examination of the specificity of the Salkowski reagent for indolic compounds produced by phytopathogenic bacteria. *Appl. Environ. Microbiol.* **61**, 793–796.

Holliday, R. (1974) Ustilago maydis. In: *Handbook of Genetics* (King, R.C., ed.), pp. 575–595. New York: Plenum Press.

Hull, A.K., Vij, R. and Celenza, J.L. (2000) *Arabidopsis* cytochrome P450 s that catalyze the first step of tryptophan-dependent indole-3-acetic acid biosynthesis. *Proc. Natl Acad. Sci. USA*, **97**, 2379–2384.

Iraqui, I., Vissers, S., Cartiaux, M. and Urrestarazu, A. (1998) Characterisation of *Saccharomyces cerevisiae ARO8* and *ARO9* genes encoding aromatic aminotransferases I and II reveals a new aminotransferase subfamily. *Mol. Gen. Genet.* **257**, 238–248.

Kahmann, R., Steinberg, G., Basse, C., Feldbrügge and Kämper, J.M. (2000) *Ustilago maydis*, the causative agent of corn smut disease. In: *Fungal Pathology* (Kronstad, J.W., ed.), pp. 347–371. Dordrecht, The Netherlands: Kluwer.

Kämper, J. (2004) A PCR-based system for highly efficient generation of gene replacement mutants in *Ustilago maydis*. *Mol. Genet. Genomics*, **271**, 103–110.

Kämper, J., Kahmann, R., Bölker, M., Ma, L.J., Brefort, T., Saville, B.J., Banuett, F., Kronstad, J.W., Gold, S.E., Müller, O., Kämper, J., Kahmann, R., Bölker, M., Ma, L.J., Brefort, T., Saville, B.J., Banuett, F., Kronstad, J.W., Gold, S.E., Müller, O., Perlin, M.H., Wösten, H.A., de Vries, R., Ruiz-Herrera, J., Reynaga-Peña, C.G., Snetselaar, K., McCann, M., Pérez-Martín, J., Feldbrügge, M., Basse, C.W., Steinberg, G., Ibeas, J.I., Holloman, W., Guzman, P., Farman, M., Stajich, J.E., Sentandreu, R., González-Prieto, J.M., Kennell, J.C., Molina, L., Schirawski, J., Mendoza-Mendoza, A., Greilinger, D., Münch, K., Rössel, N., Scherer, M., Vranes, M., Ladendorf, O., Vincon, V., Fuchs, U., Sandrock, B., Meng, S., Ho, E.C., Cahill, M.J., Boyce, K.J., Klose, J., Klosterman, S.J., Deelstra, H.J., Ortiz-Castellanos, L., Li, W., Sanchez-Alonso, P., Schreier, P.H., Häuser-Hahn, I., Vaupel, M., Koopmann, E., Friedrich, G., Voss, H., Schlüter, T., Margolis, J., Platt, D., Swimmer, C., Gnirke, A., Chen, F., Vysotskaia, V., Mannhaupt, G., Güldener, U, Münsterkötter, M., Haase, D., Oesterheld, M., Mewes, H.W., Mauceli, E.W., DeCaprio, D., Wade, C.M., Butler, J., Young, S., Jaffe, D.B., Calvo, S., Nusbaum, C., Galagan, J., Birren, B.W. (2006) Insights from the genome of the biotrophic fungal plant pathogen *Ustilago maydis*. *Nature*, **444**, 97–101.

Kepinski, S. and Leyser, O. (2003) Plant development: an axis of auxin. *Nature*, **426**, 132–135.

Kobayashi, M., Fujiwara, Y., Goda, M., Komeda, H. and Shimizu, S. (1997) Identification of active sites in amidase: evolutionary relationship between amide bond-and peptide bond-cleaving enzymes. *Proc. Natl Acad. Sci. USA*, **94**, 11986–11991.

Kriechbaumer, V., Park, W.J., Gierl, A. and Glawischnig, E. (2006) Auxin biosynthesis in maize. *Plant Biol. (Stuttg)* **8**, 334–339.

Lahey, K.A., Yuan, R., Burns, J.K., Ueng, P.P., Timmer, L.W. and Chung, K.-R. (2004) Induction of phytohormones and differential gene expression in citrus flowers infected by the fungus *Colletotrichum acutatum*. *Mol. Plant–Microbe Interact.* **17**, 1394–1401.

Magnus, V., Bandurski, R.S. and Schulze, A. (1980) Synthesis of 4–7 and 2,4–7 deuterium-labeled indole-3-acetic acid for use in mass spectrometric assays. *Plant Physiol.* **66**, 775–781.

Martínez-Espinoza, A.D., Garcia-Pedrajas, M.D. and Gold, S.E. (2002) The Ustilaginales as plant pests and model systems. *Fungal Genet. Biol.* **35**, 1–20.

Mikkelsen, M.D., Hansen, C.H., Wittstock, U. and Halkier, B.A. (2000) Cytochrome P450 CYP79B2 from *Arabidopsis* catalyzes the conversion of tryptophan to indole-3-acetaldoxime, a precursor of indole glucosinolates and indole-3-acetic acid. *J. Biol. Chem.* **275**, 33712–33717.

Moulton, J.E. (1942) Extraction of auxin from maize, from smut tumors of maize and from *Ustilago zeae*. *Botanical Gazzete*, **103**, 725–729.

Müller, A., Düchting, P. and Weiler, E.W. (2002) A multiplex GC-MS/MS technique for the sensitive and quantitative single-run analysis of acidic phytohormones and related compounds, and its application to *Arabidopsis thaliana*. *Planta*, **216**, 44–56.

Müller, P., Weinzierl, G., Brachmann, A., Feldbrügge, M. and Kahmann, R. (2003) Mating and pathogenic development of the smut fungus *Ustilago maydis* are regulated by one mitogen-activated protein kinase cascade. *Eukaryot. Cell*, **2**, 1187–1199.

Normanly, J., Grisafi, P., Fink, G.R. and Bartel, B. (1997) Arabidopsis mutants resistant to the auxin effects of indole-3-acetonitrile are defective in the nitrilase encoded by the *NIT1* gene. *Plant Cell*, **9**, 1781–1790.

Park, W.J., Kriechbaumer, V., Moller, A., Piotrowski, M., Meeley, R.B., Gierl, A. and Glawischnig, E. (2003) The Nitrilase ZmNIT2 converts indole-3-acetonitrile to indole-3-acetic acid. *Plant. Physiol.* **133**, 794–802.

Pollmann, S., Müller, A., Piotrowski, M. and Weiler, E.W. (2002) Occurrence and formation of indole-3-acetamide in *Arabidopsis thaliana*. *Planta*, **216**, 155–161.

Pollmann, S., Neu, D. and Weiler, E.W. (2003) Molecular cloning and characterization of an amidase from *Arabidopsis thaliana* capable of converting indole-3-acetamide into the plant growth hormone, indole-3-acetic acid. *Phytochemistry*, **62**, 293–300.

Robinson, M., Riov, J. and Sharon, A. (1998) Indole-3-acetic acid biosynthesis in *Colletotrichum gloeosporioides* f. sp. *aeschynomene*. *Appl. Environ. Microbiol.* **64**, 5030–5032.

Schmidt, R.C., Müller, A., Hain, R., Bartling, D. and Weiler, E.W. (1996) Transgenic tobacco plants expressing the *Arabidopsis thaliana* nitrilase II enzyme. *Plant J.* **9**, 683–691.

Sheldrake, A.R. (1973) The production of hormones in higher plants. *Biol. Rev.* **48**, 509–559.

Snetselaar, K.M. and Mims, C.W. (1994) Light and electron microscopy of *Ustilago maydis* hyphae in maize. *Mycol. Res.* **98**, 347–355.

Sosa-Morales, M.E., Guevara-Lara, F., Martínez-Juárez, V.M. and Paredes-López, O. (1997) Production of indole-3-acetic acid by mutant strains of *Ustilago maydis* (maize smut/huitlacoche). *Appl. Microbiol. Biotechnol.* **48**, 726–729.

Spaepen, S., Vanderleyden, J. and Remans, R. (2007) Indole-3-acetic acid in microbial and microorganism-plant signaling. *FEMS Microbiol. Rev.* **31**, 425–448.

Tam, Y.Y. and Normanly, J. (1998) Determination of indole-3-pyruvic acid levels in *Arabidopsis thaliana* by gas chromatography-selected ion monitoring-mass spectrometry. *J. Chromatogr. A.* **800**, 101–108.

Tanaka, H., Dhonukshe, P., Brewer, P.B. and Friml, J. (2006) Spatiotemporal asymmetric auxin distribution: a means to coordinate plant development. *Cell. Mol. Life Sci.* **63**, 2738–2754.

Tsukuda, T., Carleton, S., Fotheringham, S. and Holloman, W.K. (1988) Isolation and characterization of an autonomously replicating sequence from *Ustilago maydis*. *Mol. Cell. Biol.* **8**, 3703–3709.

Turian, G. and Hamilton, R.H. (1960) Chemical detection of 3-indolylacetic acid in *Ustilago zeae* tumors. *Biochim. Biophys. Acta*, **41**, 148–150.

Wolf, F.T. (1952) The production of indole acetic acid by *Ustilago zeae*, and its possible significance in tumor formation. *Proc. Natl Acad. Sci. USA*, **38**, 106–111.

Woodward, A.W. and Bartel, B. (2005) Auxin: regulation, action, and interaction. *Ann. Bot. (Lond.)* **95**, 707–735.

Yamada, T., Palm, C.J., Brooks, B. and Kosuge, T. (1985) Nucleotide sequences of the *Pseudomonas savastanoi* indoleacetic acid genes show homology with *Agrobacterium tumefaciens* T-DNA. *Proc. Natl Acad. Sci. USA*, **82**, 6522–6526.

Yoshida, A., Rzhetsky, A., Hsu, L.C. and Chang, C. (1998) Human aldehyde dehydrogenase gene family. *Eur. J. Biochem.* **251**, 549–557.

Zhao, Y., Christensen, S.K., Fankhauser, C., Cashman, J.R., Cohen, J.D., Weigel, D. and Chory, J. (2001) A role for flavin monooxygenase-like enzymes in auxin biosynthesis. *Science*, **291**, 306–309.

Zhao, Y., Hull, A.K., Gupta, N.R., Goss, K.A., Alonso, J., Ecker, J.R., Normanly, J., Chory, J. and Celenza, J.L. (2002) Trp-dependent auxin biosynthesis in *Arabidopsis*: involvement of cytochrome P450s CYP79B2 and CYP79B3. *Genes Dev.* **16**, 3100–3112.

SUPPLEMENTARY MATERIAL

The following supplementary material is available for this article:

Fig. S1 Verification of IPA production in response to Trp feeding in CM/Glu medium. The growth conditions were as described for Table 2. (A and B) Ethyl acetate-extracted cell-free supernatants corresponding to 100 and 200 µl of cell culture, respectively, of strain FB1 were subjected to HPLC running with gradients I (A) and II (B), respectively, as described in Experimental procedures. The IPA standard (100 nMol) was loaded as control. Absorbance was monitored at 220 nm. Retention time values are indicated above peaks. Assignment of peaks to IAA and IPA was based on retention time values (not shown for IAA) as well as reactivity with the Salkowski reagent (bottom panels). (B) The retention time value of IAA is slightly different from the one shown in Figures 3 and 4 owing to usage of a new C18 ultrasphere column (4.6 × 250 mm; 5 µm; Beckman Coulter). The additional peak at 8.0 min (marked by an asterisk) may represent a decomposition product due to the unstable nature of IPA in aqueous solutions (Sheldrake, 1973). Bottom panels: fractions (0.5 min) were collected within the indicated time range for detection of IPA (A and B) and IAA (B) with the Salkowski reagent. Absorbance was measured at 530 nm. Peak fractions from the IPA standard and the FB1 extracts are indicated by open and closed bars, respectively. (A and B) The weaker Salkowski reactions of FB1-derived IPA fractions relative to the IPA standard is reflected by lower absorbance in the HPLC profiles.

This material is available as part of the online article from:
http://www.blackwell-synergy.com/doi/abs/10.1111/j.1364-3703. 2008.00470.x
(This link will take you to the article abstract).

Please note: Blackwell Publishing are not responsible for the content or functionality of any supplementary materials supplied by the authors. Any queries (other than missing material) should be directed to the corresponding author for the article.